

# Use of noncontact dilatometry for the assessment of the sintering kinetics during mullitization of three kaolinitic clays from Cameroon

Elie Kamseu · Antonino Rizzuti · Paola Miselli ·  
Paolo Veronesi · Cristina Leonelli

Received: 5 June 2009 / Accepted: 18 August 2009 / Published online: 11 September 2009  
© Akadémiai Kiadó, Budapest, Hungary 2009

**Abstract** Noncontact dilatometry, compared to differential scanning calorimetry (DSC), was used together with scanning electron microscopy and densification behavior studies to investigate the parameters that govern the kinetics of transformation of kaolin to mullite during sintering. Three kaolinitic clays from Cameroon, with different  $\text{SiO}_2/\text{Al}_2\text{O}_3$  molar ratio, were examined. The temperatures of mullite nucleation were 973, 979, and 984 °C at 5 °C/min heating rate, respectively, for values of  $\text{SiO}_2/\text{Al}_2\text{O}_3$  molar ratio equal to 4.22, 2.22, and 2.08. At 20 °C/min heating rate, the temperatures are shifted to higher values, 992, 997, and 1,001 °C. The mullitization phenomenon, which includes a first step of nucleation and a second one of crystal growth, presented activation energy in the range of 650–730 kJ/mol, depending on the nature of the sample investigated. These values, obtained by noncontact dilatometer measurements, were comparable to those obtained by means of DSC and are in agreement with literature values. The difference in sintering kinetics for the three kaolinitic clays could explain the different morphologies obtained for the mullite grains.

**Keywords** Noncontact dilatometry · Mullite formation · Sintering kinetics · Nucleation · Crystal growth · Activation energy

E. Kamseu · A. Rizzuti · P. Miselli · P. Veronesi · C. Leonelli  
Department of Materials and Environmental Engineering,  
University of Modena and Reggio Emilia, Via Vignolesse 905,  
41100 Modena, Italy

E. Kamseu (✉)  
Local Materials Promotion Authority, MIPROMALO/  
MINRESI, 2396 Yaoundé, Cameroon  
e-mail: kamseuelie2001@yahoo.fr

## Introduction

Differential thermal analysis (DTA) and differential scanning calorimetry (DCS) have been used as rapid and convenient methods for the assessment of the kinetics of phase transformation processes and chemical reaction mechanisms during ceramics sintering [1]. For high temperature transformations of ceramic and glasses, the change in volume is measured with a thermodilatometer either in the horizontal or vertical spring-loaded pushrod geometry or in the noncontact interferometric configuration [2].

While common heating rate for DTA and TG investigations is 10 °C/min, a more appropriate heating rate for dilatometry is 3–5 °C/min. The specimen dimensions used in dilatometry are generally much larger than those used in DTA or TG; time must be allowed for heat to propagate from the specimen surface to its interior. Temperature gradients within the specimen will be more severe with increasing heating rate and specimen diameter.

Longer specimens permit higher accuracy in expansion measurements; however, they run the risk of nonuniformity of temperature along the specimen axis [2]. So, noncontact dilatometry is preferred when considerable shrinkage/expansion effect is involved because smaller specimens can be used with respect to contact pushrod dilatometers [3].

In noncontact or interferometric dilatometers, if the sample is heated, the top surface will move due to thermal expansion, and a light interference fringe shift will occur. Since it is not feasible to heat the specimen uniformly without heating the stage on which it rests, a second beam of the equipment is used to evaluate the stage expansion. So in a dual beam optical dilatometer, two visible light beams (average wavelength of 400 nm) are used and the difference in fringe shifts corresponding to the sample and

the stage represent the specimen's expansion with a resolution of 200 nm [4].

Nowadays, there are commercial equipments which work on digitalized images of the specimens. The use of two beams of light implies the use of two microscopes and two digital cameras. Focusing the image of the tip of the sample on the CCD of the camera with the maximum of the magnification achievable using visible light means that it is able to see only few hundred microns of the sample [5]. A sample of 50 mm, or 50,000  $\mu\text{m}$ , long which reaches an expansion of 1% will expand 500  $\mu\text{m}$ . Using blue light with wavelength of 478 nm and magnifying up to 0.5  $\mu\text{m}$  per pixel, the image will shift 1,000 pixels. Since the sample is free on the stage, it may move in one direction only, going out of the field of view of a video camera with 1 mega pixel (1,000  $\times$  1,000). The solution to this problem is to move the optical path to follow the expansion/contraction of the sample using two linear translation stages equipped with a step motor controlled by the computer and able to make the shift in a very short time with very high accuracy. This is the new design of the dual optical dilatometer used in this study (see details of the equipment used for this work in the Experimental part) [5].

The study of the shrinkage or expansion behavior with temperature can also be used to assess nucleation point of mullite or the point of crystallization of glasses [6–8], and in this article, we focus on the first phenomenon. The nucleation of mullite (formula:  $2\text{Al}_2\text{O}_3 \cdot 1\text{SiO}_2$ ;  $\text{SiO}_2/\text{Al}_2\text{O}_3$  molar ratio: 0.50 [2]) from kaolinitic clays (kaolin formula:  $\text{Al}_2\text{O}_3(\text{SiO}_2)_2 \cdot 2\text{H}_2\text{O}$ ;  $\text{SiO}_2/\text{Al}_2\text{O}_3$  molar ratio: 2 [2]), as other sintering of ceramic raw materials, are considered first-order reaction where densification is accompanied by reduction in specimen's dimensions and decrease in porosity. The decrease in density is due to the transformation at 980–1050  $^\circ\text{C}$  of the spinel/alumina with density of 2.67–2.80  $\text{g}/\text{cm}^3$  to highly dense mullite grains (3.17  $\text{g}/\text{cm}^3$ ) [2].

The use of the Kissinger theory for kaolin–mullite sintering in the context of this study is based on the consideration that mullite is the essential crystallization product and responsible for the maximum peak in the case of DSC and the regime of constant linear shrinkage near the temperature of mullitization for the optical dilatometry analysis.

The shrinkage rate,  $d(dL/L_0)/dt$ , can be expressed as [6–11]:

$$\frac{d(dL/L_0)}{dt} = A_0 T^a \exp\left[\frac{-E_{\text{sin}}}{RT}\right] \left[\frac{dL}{L_0}\right]^{1-n/2} \quad (1)$$

where  $dL/L_0$  is the linear shrinkage,  $t$  is the time (s),  $A_0$  is the Arrhenius pre-exponential factor at a constant particle size,  $R$  is gas constant (8.314  $\text{J mol}^{-1} \text{K}^{-1}$ ),  $T$  is the

absolute temperature (K),  $E_{\text{sin}}$  is the activation energy for sintering ( $\text{J mol}^{-1}$ ), and  $a$  and  $n$  are constants depending on the transport mechanism.

Assuming that the sintering of kaolinitic clays follows the viscous flow mechanism,  $a = 0$  and  $n = 2$  and Eq. 1 can be rewritten as:

$$\frac{d(dL/L_0)}{dt} = A_0 \exp\left[\frac{-E_{\text{sin}}}{RT}\right] \quad (2)$$

In nonisothermal conditions, at a constant heating rate  $v$  ( $^\circ\text{C}/\text{min}$ ) and after integration of Eq. 2 becomes:

$$\ln\left(\frac{v}{T_x^2}\right) = \left(\frac{-E_{\text{sin}}}{RT_x}\right) \quad (3)$$

where  $T_x$  is the temperature at which the sintering process attains a constant shrinkage value  $X$ . A plot of  $\ln(v/T_x^2)$  versus  $1/T_x$  in the case of dilatometric curves at different heating rates should give a straight line whose slope is  $E_{\text{sin}}/R$ . The temperatures of the mullitization peak ( $T_P$  for  $T_x$ ) for each heating rate were used for DSC, while those of constant shrinkage near the mullitization peak were used for dilatometry.

The study was performed on three kaolinitic clays from Cameroon with different  $\text{SiO}_2/\text{Al}_2\text{O}_3$  ratios which developed during the sintering orthorhombic crystals of mullite, space group *pbam*, as major phase [12]. Mullite grains presented an average alumina to silica molar ratio of 2:1 but it was found that the microstructure of the firing product can be described as interlocking of secondary (types II and III) elongated mullite crystals with cuboid primary mullite (type I) with alumina to silica ratio varying from 1:1 to 2–5:2 being dependent on the raw composition and impurities.

The dilatometric and DSC curves discussed in this article aim to complete the morphological and mineralogical studies presented elsewhere and, at the same time, this investigation wants to state the effect of heating rate in an optical noncontact dilatometer on the mullite formation. In fact, as per author's knowledge, there are no studies of mullite formation performed with noncontact dilatometer reported in literature. This important investigation technique is more and more diffused in the industrial ceramic labs and has not received much attention from researchers when mullitization or other ceramic body transformations are involved.

## Materials and experimental methods

### Materials

The raw materials investigated in this study are three kaolinitic clays from Ntamuka (TAN), Mayouom (MAY),

and Wabane (WAB), all localities situated in the hills of western Cameroon [13]. Apart from the principal mineral, kaolin, the presence of  $\alpha$ -quartz was recorded as second crystalline phase. The chemical composition, as detected by ICP-AES spectroscopy, has been reported elsewhere [12], but roughly they have the following composition: TAN:  $62\text{SiO}_2\text{-}25\text{Al}_2\text{O}_3\text{-}1.5$  (monovalent, divalent cations, iron and titanium oxides); MAY:  $44\text{SiO}_2\text{-}34\text{Al}_2\text{O}_3\text{-}1.7\text{Fe}_2\text{O}_3\text{-}4.4\text{TiO}_2$ , traces of monovalent and divalent cation oxides; and WAB:  $43\text{SiO}_2\text{-}35\text{Al}_2\text{O}_3\text{-}4.8\text{TiO}_2\text{-}1.7$  (monovalent, divalent cations, iron oxides) (wt%). The remaining part is loss of ignition, i.e., water, carbonates, hydroxides, and organic matter. The main difference, apart from the presence of impurities, is the  $\text{SiO}_2/\text{Al}_2\text{O}_3$  molar ratio equal to 4.22, 2.22, and 2.08 for TAN, MAY, and WAB, respectively. MAY and WAB possess very similar silica to alumina ratio and developed more elongated Al-rich mullite, especially in regions of concentration of glassy film [12].

The study [12] of the structural parameters of mullite and grain size as a function of temperature indicated that grain growth were preferentially on the *c* direction with a maximum in the temperature range between 1400 and 1500 °C where larger grains of mullite were found.

Between 1200 and 1300 °C, the formation of  $\text{TiO}_2$  and  $\text{Al}_2\text{O}_3\cdot\text{TiO}_2$ , tialite, crystals was responsible for the presence of fissures or cracks. In WAB,  $\text{TiO}_2$  crystals decreased progressively with temperature development. Both these two Ti-rich crystals seem to be unstable with temperature.

If mullite remains the main phase in the microstructure of the three kaolinitic clays, the additional second or third phases influence [5] the microstructure as well as the mechanical properties the final product.

The development of more cristobalite (30%) in the TAN clay conduct to the mullite-cristobalite system, while the formation of Ti–Al phase influenced the mullite system for the samples MAY and WAB. These results are indicative for the possible application of the three kaolinitic clays in the area of ceramic, refractories, and others engineering materials.

## Methods

Sintering behavior was monitored by a noncontact dilatometer (ESS MISURA HSM ODHT model 1600/80, Expert System Solutions, Modena, Italy). The apparatus works with a double beam system that acquires images of the top part of the specimen as well as the bottom part to acquire linear deformation lengthwise and to avoid the false measurement of the dilatation of the stage. Unlike electronic dilatometers, the resolution of an optical dilatometer cannot be less than 0.1  $\mu\text{m}$  because it is limited by the wavelength of the light. The optical dilatometer can

give reproducible results with a resolution of 1  $\mu\text{m}$ , over a sample length of 15 mm, which is 1 part over 15,000. This resolution may be considered too low, but it becomes valuable for a sintering process where the size variation may reach several percentage points [14]. One relevant feature of this kind of dilatometers is the fact that the calibration curve is not necessary once the magnification of the two optical paths is carefully established (in this study: by the producer against a Standard Reference Material supplied by NIST).

Specimens are prepared by gently pressing the clay powders in a cylindrical mold of the size: 15 mm height and 5 mm diameter. Heating rates used were: 5, 10, 15, and 20 °C/min for studying the densification process up to 1,300 °C. It has to be reminded that the absence of the pushrod allows the free-standing specimen to expand without contrasting any pressure.

Similarly pressed specimens were used for Pt crucibles of a DSC apparatus (DSC 404 Netzsch, Selb, Germany) operated from 20 to 1,400 °C at the same heating rates used for the dilatometer. Calcined kaolin was used as reference material.

The measurements were repeated at least twice for each sample to ensure reproducibility of the results. The experimental data were used to elaborate the kinetics parameters as described above.

## Results and discussion

Thermal behavior as a function of temperature and heating rate

It is well known [11] that there is a strong effect of the heating rate on the thermal transformation of raw materials for ceramics, among these clays and kaolins are included. Figure 1a–c shows these effects as collected in a noncontact dilatometer for the three kaolinitic clays investigated in this study.

All the samples undergo a slight expansion up to 560–600 °C, poorly influenced by the heating rate, then a rapid shrinkage, highly dependent on heating rate, then a slow shrinkage up to 1,000 °C, where a second rapid shrinkage is recorded. Then, a plateau in the dilatometric curve up to 1,250–1,300 °C is observed in most cases, followed by a sharp shrinkage which takes the data to run out of scale.

The first slight expansion of clay is well known to be due to the expansion of  $\alpha$ -quartz present in the clay. The average thermal expansion is 0.3% with minor influence of heating rate for MAY and WAB, while it is slightly more, 0.5%, for TAN. The calculated coefficient of expansion in the dehydroxylation interval, 20 to 500–600 °C, depends on the heating rate (Fig. 1). For samples MAY and WAB,

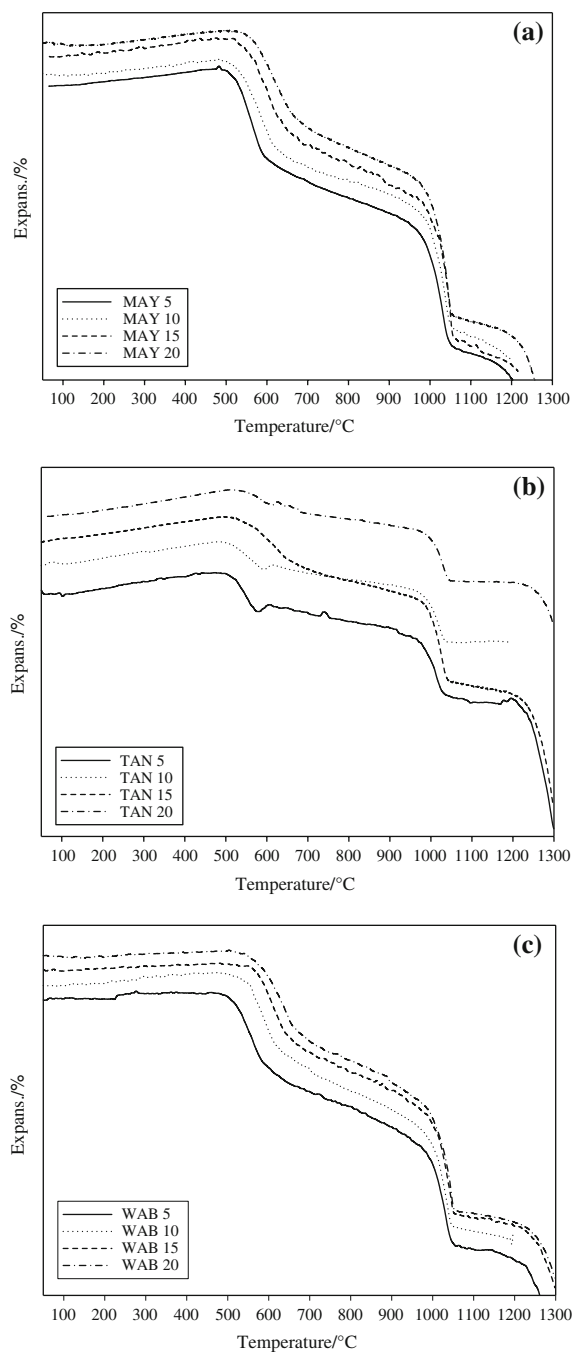


**Fig. 1** Noncontact thermal dilatometry as a function of temperature of the three kaolinitic clays: **a** MAY (MAY5 = 5 °C/min, MAY10 = 10 °C/min, MAY15 = 15 °C/min, MAY20 = 20 °C/min). **b** TAN (TAN5 = 5 °C/min, TAN10 = 10 °C/min, TAN15 = 15 °C/min, TAN20 = 20 °C/min). **c** WAB (WAB5 = 5 °C/min, WAB10 = 10 °C/min, WAB15 = 15 °C/min, WAB20 = 20 °C/min)

the expansion rate decreases from  $5.91 \times 10^{-6}$  and  $8.61 \times 10^{-6} \text{ K}^{-1}$  at 5 °C/min to  $5.50 \times 10^{-6}$  and  $4.12 \times 10^{-6} \text{ K}^{-1}$  at 20 °C/min, respectively (Table 1). TAN presents an expansion rate which is almost the double, being  $9.09 \times 10^{-6} \text{ K}^{-1}$  at 5 °C/min and  $9.78 \times 10^{-6} \text{ K}^{-1}$  at

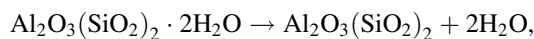
**Table 1** Variation of the expansion coefficient due to quartz ( $\alpha_q$ ) and the coefficient of shrinkage due to the dehydroxylation of kaolinitic clays and formation of mullite ( $\alpha_m$ ) as a function of sintering rate

Samples	$\alpha/10^{-6} \text{ K}^{-1}$	5 °C/min	10 °C/min	15 °C/min	20 °C/min
MAY	$\alpha_q$	5.91	5.55	5.57	5.50
	$\alpha_m$	-49.55	-43.50	-49.41	-49.85
TAN	$\alpha_q$	9.09	9.24	8.29	9.78
	$\alpha_m$	-27.64	-20.31	-20.89	-16.73
WAB	$\alpha_q$	8.61	8.61	4.76	4.12
	$\alpha_m$	-88.56	-89.95	-85.46	-91.31

*Note:*  $\alpha_q$  is relative to the expansion of quartz, while  $\alpha_m$  is relative to the shrinkage that characterizes the crystallization of mullite

20 °C/min. These values can be explained taking into account the highest content of free  $\alpha$ -quartz present in TAN clay with respect the other two raw materials investigated.

The dehydroxylation reaction,



responsible for the sharp decrease in size (1.5–3%) of all the samples is also visible in the DSC curves which present an endothermic peak centered around 550–600 °C (Fig. 2). The shrinkage, due to the loss of OH groups bonded to the kaolinitic mineral structure, starts at lower temperatures if low heating rate is adopted: at 5 °C/min the shrinkage starts at 520, 524, and 514 °C for WAB, MAY, and TAN, respectively. The effect of the heating rate is not the same for all the three clays, increasing of about 25–30 °C for 20 °C/min, and moreover, the overall shrinkage is also dissimilar. According to previous studies [15–18], the complexity of this process is linked to the nature of the kaolinite mineral,  $\text{SiO}_2/\text{Al}_2\text{O}_3$  ratio, impurities, crystallinity, and others. It has to be noted that the presence of impurities takes along free water molecules which are not as strongly linked to the kaolin planes as the hydroxyl groups. This is the case of WAB clay which presents the highest impurities content and the highest shrinkage value,

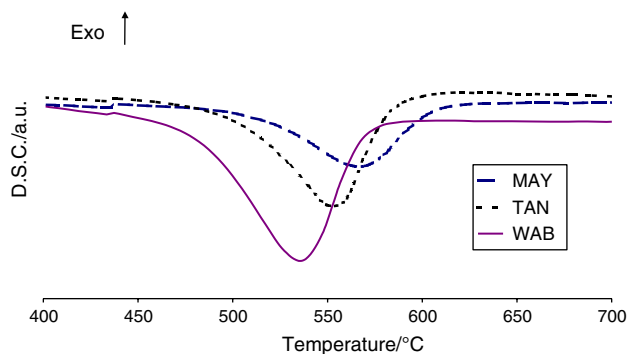


**Fig. 2** DSC peaks of dehydroxylation as a function of the temperature at a fixed heating rate of 10 °C/min for the three kaolinitic clays

close to 3%, when compared to the other two clays. Since dehydroxylation process is complicated by gas-transport in addition to heat-transport phenomenon [19], no further studies will be present in this paper. The kinetic studies will be performed only on spinel to mullite transformation process being characterized only by heat-transport.

In the temperature range 980–1,050 °C, the transformation of spinel/alumina into high-density mullite starts (compare Figs. 1 and 3) [12]. Even though the process is complex, according to different authors [20, 21], a spinel phase can be speculated before the mullite crystal formation; the temperature at which the shrinkage is recorded in Fig. 1a–c is slightly affected by heating rate. The dilatometric mullitization shrinkage onset points for the three clays are as follows:

for MAY 1,045 °C at 5 °C/min and 1,051 °C at 20 °C/min;  
for WAB 1,045 °C at 5 °C/min and 1,057 °C at 20 °C/min; and  
for TAN 1,053 °C at 5 °C/min and 1,061 °C at 20 °C/min.

The slope of the dilatometric curve, i.e., the shrinkage rate, is very slightly affected:

for MAY  $-49.55 \times 10^{-6} \text{ K}^{-1}$  at 5 °C/min and  $-49.85 \times 10^{-6} \text{ K}^{-1}$  at 20 °C/min;  
for WAB  $-88.56 \times 10^{-6} \text{ K}^{-1}$  at 5 °C/min and  $-91.31 \times 10^{-6} \text{ K}^{-1}$  at 20 °C/min; and  
for TAN  $-27.64 \times 10^{-6} \text{ K}^{-1}$  at 5 °C/min and  $-16.73 \times 10^{-6} \text{ K}^{-1}$  at 20 °C/min;

the dilatometric curves almost overlapped. One exception is clay TAN, where the absence of a sufficient amount of impurities did not help mullite nucleation [20, 21] joined to a high  $\alpha$ -quartz refractory crystal content. The overall shrinkage at 1,200 °C for TAN is only 1.8%, while that for MAY and WAB is 3.5 and 7.2%, respectively.

The DSC tracks are instead very much affected by the heating rate, with the following shifts of the onset crystallization peak for the mullite crystals:

for MAY 979 °C at 5 °C/min and 992 °C at 20 °C/min;  
for WAB 984 °C at 5 °C/min and 1,001 °C at 20 °C/min; and  
for TAN 973 °C at 5 °C/min and 992 °C at 20 °C/min.

For dilatometric curves as well as for the DSC curves, the intermediate heating rate, between 5 and 20 °C/min, give intermediate values (Figs. 1, 3).

To summarize the effect of heating rate on the sintering behavior of the three clays investigated, it can be stated that the dehydroxylation is the process which is more affected, the water vapor exit from the ceramic body is very sensitive to local temperature. Higher heating rate produces a

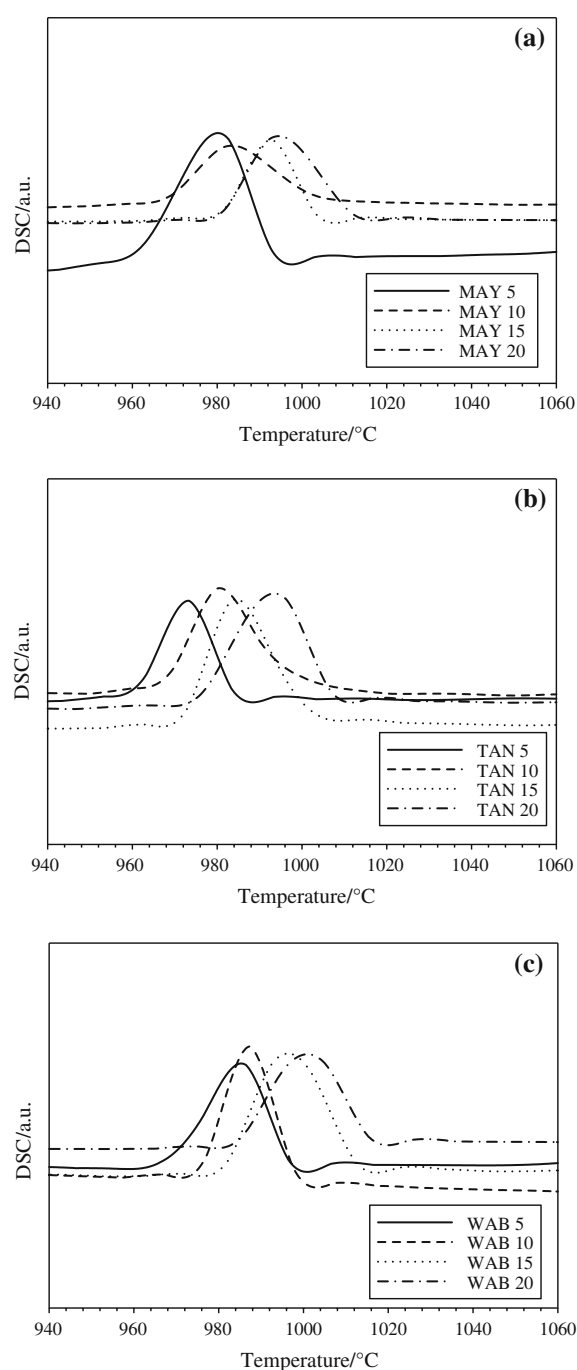


**Fig. 3** Variation of DSC mullitization exothermal peaks as a function of heating rate for: **a** MAY. **b** TAN. **c** WAB

gradient in the sample corresponding to a gradient in evaporation and hence in the shrinkage.

The shrinkage corresponding to mullite formation is basically a nucleation rate-controlled mechanism with  $\text{Al}^{3+}$  and  $\text{Si}^{4+}$  diffusion. The short diffusion path of both cations is not so much affected by temperature gradients as the dehydroxylation processes; moreover, this is a proof that inhomogeneous sintering/mullitization is not created even



at high heating rates in the noncontact dilatometer. Nevertheless, the more sensitive DSC apparatus recorded a temperature peak shift wider than that recorded by the dilatometer using the same heating rates.

### Mullite crystallization kinetics

The mullite crystallization kinetics was studied using dilatometric (Fig. 1) and DSC data (Fig. 3).

As mentioned above and proved in our previous work [12], the transformation at 980–1,050 °C of the spinel/alumina (with density of 2.67–2.80 g/cm<sup>3</sup>) to highly dense mullite grains (3.17 g/cm<sup>3</sup>) is accompanied by the stages of nucleation and growth of mullite needles. Mullite needles grow up to 0.3 μm (compare also results from [22, 23]) below 1,400 °C, but from this point to 1,500 °C, they grow very rapidly without any further shrinkage. Moreover, the mullite crystals formed belong to the same symmetry (orthorhombic, space group: *pbam*) while possessing variable SiO<sub>2</sub>/Al<sub>2</sub>O<sub>3</sub> ratio.

According to our Rietveld quantitative analysis on the three clays, the wt% of mullite was 18 and 19 for MAY and WAB, respectively, at 1,100 °C and only 10 wt% for TAN at 1,200 °C (lower temperature at which mullite was determined quantitatively in this sample).

In summary, the mullite formed in WAB and MAY is approximately two times the mullite content of TAN, as could be deduced also by the overall shrinkage values reported in the previous chapter.

For the three kaolinitic clays under study, the activation energy for mullitization,  $E_a$ , was evaluated graphically by plotting Eq. 3 in terms of  $\ln(v/T_x^2)$  versus  $1000/T_x$  for the nonisothermal dilatometric measurements (Fig. 4). The calculated activation energy values were  $687 \pm 117$ ,  $649 \pm 85$ , and  $731 \pm 111$  kJ/mol, respectively, for TAN, MAY, and WAB. The values obtained applying the DSC nonisothermal method were  $657 \pm 100$ ,  $671 \pm 108$ , and  $723 \pm 113$  kJ/mol in the same sequence (Fig. 5). The error in the calculation is similar in the two methods used, dilatometry and DSC.

The apparent activation energy for the transformation process of kaolin determined by a nonisothermal method proposed by Ligerio et al. [24] and based on Johnson–Mehl–Avrami theory was equal to  $730 \pm 150$  kJ/mol value also reported in [25] for kinetic studies of mullitization of sol-gel precursors using dynamic X-ray diffraction and DTA.

When we compare two clays with similar SiO<sub>2</sub>/Al<sub>2</sub>O<sub>3</sub> ratio, WAB with 2.08 and MAY with 2.22, we can recognize the effect of impurities lowering  $E_a$  for MAY by decreasing liquid phase viscosity [7, 8].

Even though orthorhombic crystals of mullite were identified as major phase developed during the sintering of three kaolinitic clays, as stated above, MAY and WAB

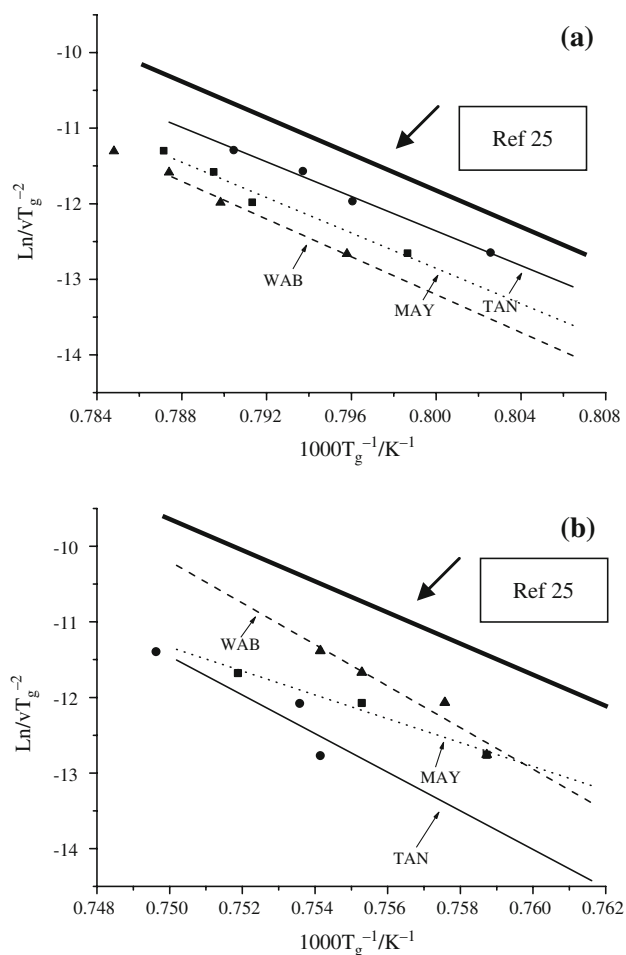


**Fig. 4** a Variation of  $\ln(v/T_p^2)$  as a function of  $1/T_p$  (DSC). b Variation of  $\ln(v/T_x^2)$  as a function of  $1/T_x$  (noncontact dilatometry)

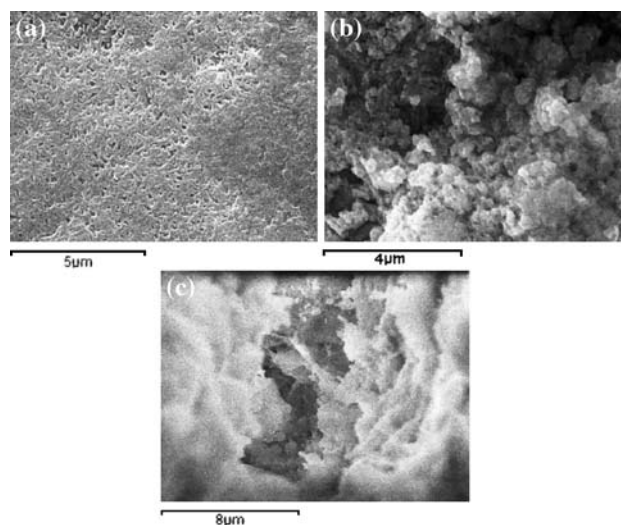


**Fig. 5** Micrographs of mullite grains in different samples at 1,300 °C. a MAY. b WAB. c TAN

developed more elongated Al-rich mullite, especially in regions of concentration of glassy film, and TAN presented more needle-shaped mullite grains already at 1,200 °C (Fig. 5). The mullite crystals have also been observed at higher temperatures than those investigated in this study (studies up to 1,500 °C are reported in [22]) and the tendencies have been confirmed.

## Conclusions

The sintering kinetics of mullite crystals during thermal treatment of three kaolinitic clays from Cameroon was studied. This study is probably the first one that approached the sintering behavior of clay minerals with a dilatometer using different heating rates. Pushrod dilatometers are usually operated at one optimum heating rate due to the compromise between specimen length (the longer the specimen the more precise the measurement) and heat gradient (the longer the specimen the less homogenous is the sintering). In the case of the optical dilatometer used for this study, operating with a dual beam, the precision and accuracy has been proved to be close to that of a DSC apparatus (same activation energy values and transformation temperatures) within the range of heating rate used: from 5 to 20 °C/min. The specimens' dimensions (15 mm height) are small enough to be assured a homogeneous heating, hence sintering, from room temperature to 1,300 °C. Reproducibility of the sintering curves obtained with the dilatometer at different heating rates is proven by the fact that same shrinkage temperatures and rates have been recorded for the mullitization process.

Following conclusions were drawn from the experimental results:

- The temperature of crystallization of mullite varies from 973 to 1,001 °C, varying the SiO<sub>2</sub>/Al<sub>2</sub>O<sub>3</sub> molar ratio, the impurities content, and the heating rate.
- The activation energy of the crystallization of mullite calculated in nonisothermal conditions using either DSC or noncontact dilatometry was in the range of 650–730 kJ/mol in good agreement with literature.
- Kinetic studies demonstrated that noncontact dilatometry is an adequate method for the study of the crystallization of mullite as sensitive as DSC.

## References

1. Kamseu E, Leonelli C, Boccaccini DN. Non-contact dilatometry of hard and soft porcelain compositions. *J Therm Anal Calorim.* 2007;88(2):571–6.
2. Kingery WD, Bowen HK, Uhlmann DR. *Introduction to ceramics.* 2nd ed. New York: Wiley; 1976.
3. Raether F, Hofmann R, Muller G, Solter HJ. A novel thermo-optical measuring system for the in situ study of sintering processes. *J Therm Anal Calorim.* 1998;53:717–35.
4. Paganelli M. Using optical dilatometer to determine sintering behaviour. *Am Ceram Soc Bull.* 2002;81(11):25–30.
5. Boccaccini AR, Hamann B. Review in situ high-temperature optical microscopy. *J Mater Sci.* 1999;34:5419–36.
6. Karamanov A, Aloisi M, Pelino M. Sintering behaviour of glass obtained from MSWI ash. *J Eur Ceram Soc.* 2005;25:1531–40.
7. Romero M, Martín-Márquez J, Rincon JMa. Mullite formation kinetic from a porcelain stoneware body for tiles production. *J Eur Ceram Soc.* 2006;26(9):1647–52.
8. Traorè K, Gridi-Bennadji F, Blanchart P. Significance of kinetic theories on the recrystallization of kaolinite. *Thermochim Acta.* 2006;451:99–104.
9. Sestak J. *Thermophysical properties of solids—their measurements and theoretical thermal analysis.* Prague: Academia; 1984.
10. Chen H. A method for evaluating viscosities of metallic glasses from the rates of thermal transformations. *J Non-Cryst Solids.* 1978;27:257–63.
11. Brown E. *Handbook of thermal analysis and calorimetry.* Amsterdam: Elsevier; 1998.
12. Kamseu E, Braccini S, Corradi A, Leonelli C. Microstructural evolution during thermal treatment of three kaolinitic clays from Cameroon. *Adv Appl Ceram.* 2009;108(6):338–46.
13. Njoya A, NKoumbou C, Grosbois C, Njopwouo D, Njoya D, Courtin-Nomade A, et al. Genesis of Mayouom kaolin deposit (western Cameroon). *Appl Clay Sci.* 2006;32:125–40.
14. Paganelli M. Sintering behaviour of clays for the production of ceramics. *cfi/Ber. DKG* 2007;84(5):E1–3, see also [www.expertsolutions.com](http://www.expertsolutions.com).
15. Murray P, White J. Interpretation of the differential thermal analysis of the clay minerals. Part IV: kinetics of the thermal dehydration of clays. *Trans Br Ceram Soc.* 1955;54:137.
16. Castelein O, Soulestin B, Bonnet JP, Blanchart P. The influence of heating rate on the thermal behaviour and mullite formation from a kaolin raw material. *Ceram Int.* 2001;27:517–22.
17. Schumucker M, Hildmann B, Schneider H. Mechanism of 2/1- to 3/2-mullite transformation at 1650 °C. *Am Mineral.* 2002; 87:1190–3.
18. Takei T, Kameshima Y, Yasumori A, Okada K. Crystallisation kinetics of mullite in alumina-silica glass fibers. *J Am Ceram Soc.* 1999;82(10):2980–7.
19. Paulik F. Transformation-governed heating techniques in thermal analysis I. *J Therm Anal Calorim.* 1999;58:711–23.
20. Chen CY, Tuan CS. Microstructural evolution of mullite during the sintering of kaolin powder compacts. *Ceram Int.* 2000; 26:715–20.
21. Ribeiro MJ, Tulyagavov DU, Ferreira JM, Labrincha JA. High temperature mullite dissolution in ceramic bodies derived from Al-rich sludge. *J Eur Ceram Soc.* 2005;25:703–10.
22. Leonelli C, Kamseu E, Melo UC, Corradi A, Pellacani GC. Mullitization behaviour during thermal treatment of three kaolinitic clays from Cameroon: densification, sintering kinetics and microstructure. *Interceram.* 2008;57(6):396–401.
23. Lu HY, Wang WL, Tuan WH, Lin MH. Acicular mullite crystals in vitrified kaolin. *J Am Ceram Soc.* 2004;87(10):1843–7.
24. Ligeró RA, Vazques J, Casas-Ruiz M, Jiménez-Garay R. A study of the crystallization kinetics of some Cu–As–Te glasses. *J Mater Sci.* 1991;6:211–5.
25. Zhao H, Hiragushi K, Mizota Y. Mullite formation of colloidal matrix hybrid aluminosilicate gel. *J Sol–Gel Sci Technol.* 2003;27:287–91.